Effects of codoping on the ferromagnetic enhancement in ZnO

Sergey Lisenkov, Antonis N. Andriotis, R. Michael Sheetz, and Madhu Menon

Effects of co-doping on the ferromagnetic enhancement in ZnO

Sergey Lisenkov*

Department of Physics, University of South Florida Tampa, FL 33620-5700

Antonis N. Andriotis†

Institute of Electronic Structure and Laser, FORTH, P.O. Box 1527, 71110 Heraklio, Crete, Greece

R. Michael Sheetz‡

Center for Computational Sciences, University of Kentucky, Lexington, KY 40506-0045

Madhu Menon§

Department of Physics and Astronomy, University of Kentucky, Lexington, KY 40506-0055
Center for Computational Sciences, University of Kentucky, Lexington, KY 40506-0045

The present work investigates the effect of the anionic co-doping on the magnetic properties of the DMSs doped with transition metal (TM) ions, namely that of Zn(Mn,X)O, X=C,N,P and S. The present findings are in complete analogy with the corresponding results for the cationic co-doping of Zn(TM$_1$,TM$_2$)O as studied in our earlier works. For both, the cationic and anionic co-dopings, we find that the magnetic impurities induce magnetic moments on their nearest neighbors with the largest induced magnetic moment observed on the cation or the anion which mediates two magnetic impurities. The magnetic interaction in the case of the anionic co-doping can be seen as a double exchange or a superexchange type of mechanism. On the other hand, in the cationic co-doping, the magnetic interactions take the form of a double-exchange or a superexchange between polarized tetrahedra each centered at one of the co-dopants.

I. INTRODUCTION

Dilute magnetic semiconducting (DMS) materials belonging to groups III-V and II-VI are of immense interest for applications in electronic and magnetic devices. These materials are known to become ferromagnetic (FM) as a result of doping or co-doping (simultaneous doping of two different atoms) with transition metal (TM) atoms. Most studied among the DMS host materials are doped ZnO and GaN due to the prediction of FM above room temperature for these materials[1,2].

As a DMS host ZnO has considerable appeal owing to its multifunctionality. These include a wide band gap of 3.3 eV[3] and therefore wide applications in optoelectronic industry[4], strong piezoelectricity[5] and usefulness in field effect transistors[6].

This has led to a large number of experimental[7–13] and theoretical[14–19] studies of TM doped ZnO. There is considerable controversy regarding the experimental values reported for Curie temperature and magnetization, however. For example, in the case of Mn-doped ZnO, some experiments report above room temperature FM[11,20], while others report low temperature FM[10,21]. Electron Paramagnetic Resonance (EPR) measurements has led to the conclusion that the observed magnetic signal from n-type samples of Co^{++}-doped ZnO [to be denoted as Zn(Co)O] should be attributed to states other than the $3d^7$-Co states[22], while Magnetic Circular Dichroism (MCD) has shown that room-temperature FM in Zn(Co)O could be attributed to the hybridization of the conduction band of the doped ZnO with some of the d-electrons of the magnetic ions[23].

On the other hand, the origin of magnetism in the TM-doped ZnO is far from well understood. This is further complicated by the fact that some TM dopants (e.g., Co) lead to n-type doping while others lead to p-type (e.g., Mn). It is worth noting that Mn^{+2} doping into ZnO does not by itself generate p-type carriers; these must be introduced deliberately by other routes[13]. There is no direct test of Dietls's p-type predictions for the magnetism in Zn(Mn)O. There is ,however, indirect experimental evidence of p-type conductivity in Zn(Mn)O (see Kittilstved *et al*[13]).

Magnetism was observed in ZnO doped with most of the $3d$-elements among which the magnetism of the low-doped Zn(Mn)O leads to the conclusion that it can be induced by either localized defect states or band states[23]. Several theoretical approaches have concluded that doping with Mn atoms does not lead to FM ground state in ZnO and suggesting the necessity of co-doping to stabilize FM in Mn doped ZnO[24–28]. Recent experimental works have shown FM stabilization in Al co-doped Zn(Co)O which was attributed to the extra electrons supplied by Al[29].

Xu *et al.*[30] showed that FM is greatly enhanced in bulk Zn(Mn)O when co-doped with Al. In particular, for 2% Mn concentration, the magnetic moment per Mn atom exhibits a non-monotonic increase when co-doped with Al.

This increase starts from vanishing values of the magnetic moment per Mn atom at zero Al-concentrations, peaks at about 1% Al-concentration with a value as high as 4.5 μ_B and drops to smaller magnetic moment values as the Al concentration keeps increasing. For these samples, at the 1% Al-concentration, the the ratio of the carriers density (n_c) to that of the magnetic ions (n_i) is ≈ 0.5.

It is worth noting, however, that in the case of Zn(Mn)O-films a significant increase in the magnetic moment per Mn atom was observed as compared to the bulk even with no co-dopants[31].

One of the earliest attempts to enhance the FM in Zn(Mn)O was to co-dope it with N. In a DFT/GGA-based theoretical investigation, Wang *et al.*[24] showed that Mn and N like to coexist as nearest neighbors in ZnO; the resulting hybridization between N($2p$) and Mn($3d$) orbitals was found to be the cause of a FM ground state. This was attributed to the polarization the Mn atoms impose on the N atoms with the latter oriented in AFM configuration with respect to its Mn neighbors. In the case when the magnetic moments of Mn and N are parallel, the Mn-Mn interaction (of the Mn-N-Mn chain) becomes AFM. One interesting result of this work is that O- and Mn-atoms do not contribute states at the Fermi energy despite the hybridization that develops between them.

Similarly, nitrogen has been found to enhance FM in Zn(Mn)O and suppress that of Zn(Co)O[13]. In the absence of N (i.e., absence of p-type dopants), the Mn(t_{2g}) are highly localized. This is consistent with the measured S=5/2 Curie-Weiss paramagnetism in the absence of N. However, at sufficiently high N-concentrations, one of the Mn(t_{2g}) electrons becomes delocalized partially into the impurity band formed by the N shallow acceptors stabilizing FM either as Zener-type or double exchange. For n-type Zn(Mn)O, the carriers will not delocalize onto Mn^{2+} due to the large exchange energy of Mn^{2+} (see Ref.[13] and references therein).

In our previous investigation we studied the magnetic features of the ZnO and GaN systems both co-doped by two TMs with the latter substituting cations. The present work completes our investigation by studying substitutional doping of ZnO at both anionic and cationic sites. In particular, in this paper, we present our results of a systematic theoretical study of co-doped ZnO, with the goal of understanding the nature and origin of the magnetic interactions in this system. We first explore the effects of substitutional doping with Mn atoms (Mn substituting Zn). We denote this system by Zn(Mn)O. Next, we calculate the effects of additional anionic dopant or vacancy impurities and investigate the FM enhancement and make predictions for the preferred magnetic configurations of pairs of different ion types for this enhancement. Our main finding is that while the FM state is not favored in the Zn(Mn)O systems, co-doping provided by an additional dopant or vacancy leads to the development and stabilization of FM.

The presentation outline of this paper is as follows. In the next section we describe our computational approach and justify its applicability to the co-doped ZnO. In Sec. III, we present our computational results for ZnO with multiple Mn dopings. This is followed by results for co-doped Zn(Mn)O with various elements in Sec. IV. Finally, we summarize our results in Sec. V.

II. SYSTEM AND COMPUTATIONAL DETAILS

The co-doped ZnO systems are simulated by a relatively large 72 atom supercell in a wurzite structure. Mn atoms are used to substitute Zn in ZnO to simulate the Zn(Mn)O system. Co-doping is accomplished by an additional substitution of the O atom to obtain Zn(Mn,X)O system with X = C, N, P, and S. The vacancy co-doping is simulated by removing an O atom from Zn(Mn)O. In Fig. 1 we show a 72 atom Zn(Mn)O supercell with 4 Mn atoms replacing 4 widely separated Zn atoms in "far" configuration. In all configurations considered we calculate the energy difference between FM and antiferromagnetic (AFM) ordering, $\Delta E = E_{FM} - E_{AFM}$ (energy difference defined per supercell) for determining the magnetic stability ($\Delta E < 0$ indicates FM to be favorable).

For the co-doped ZnO systems studied we used first-principles density functional theory (DFT) in the spin polarized generalized gradient approximation (SGGA) and the Perdew-Burke-Ernzerhof (PBE)[32] augmented by including Hubbard-U corrections based on Dudarev's approach[33] as implemented in the Vienna Ab-initio Simulation Package (VASP)[34–36]. The U values were selected from our earlier works and are: $U_{d;Zn}=10.5$ eV, $U_{d;Mn}=5.0$ eV and $U_{p;O}=7.0$ eV. The U values for all the anionic dopants, X=S, N, C, P, were set to zero, ie., $U_{p;X}=0.0$ eV. Calculations were later repeated for U$\neq$0 for these anionic dopants for checking the dependence of the results on U. We chose a value of $U_{p;X}=8.0$ eV for X=S, N, C, P. The projected augmented wave (PAW) potential[35,36] is used to describe the core electrons. After testing for convergence we settled for a $3\times6\times2$ Γ-centered pack for **k**-vectors sampling. A kinetic energy cutoff of 550 eV was found to be sufficient to achieve a total energy convergence of the energies of the systems to within 1 meV. Gaussian smearing of 0.05 eV was chosen to accelerate electronic convergence. The optimization of atomic positions (including full cell optimization) was allowed to proceed without any symmetry constraints until the force on each atom is less than 5 meV/Å.

III.   MAGNETIC PROPERTIES OF MN DOPED ZNO

We investigate the magnetic properties of $Zn(Mn_x)O$ system with up to 4 Mn dopings (Mn replacing Zn atom). In each of these cases we fully optimize the supercells by allowing individual atomic positions and the cell volume to vary. Contrary to $Zn(Co)O$ which does not exhibit significant volume change upon Co-doping, $Zn(Mn)O$ shows volume changes according to Vegard's law upon Mn-doping[37]. We point out that the relaxation of the cell volume is extremely critical for an accurate estimation of the magnetic ground state since in many cases the difference, E_{FM}-E_{AFM}, can be small and therefore a change in the cell volume can easily flip the sign of the energy difference.

We first explore the relative stabilities of each of the Mn_x (x=2, 3 and 4) cases by considering Mn substitutions at Zn sites that are not nearest neighbors ("far") and comparing to those with Mn forming nearest neighbors ("near"). We define the energy difference, $\Delta E=E_{near}$-E_{far}, as the difference between the energy of the most favorable spin configuration of the *near* case from the energy of the most favorable spin configuration of the *far* case. Our calculated energy differences are shown in Fig. 2 and support the earlier findings by other groups that Mn atoms prefer to cluster together in ZnO[24,25]. Furthermore, there is a monotonic increase in this energy difference as the number of Mn atoms increases.

The lowest energy configurations for all $Zn(Mn_x)O$ considered were non-FM. In Table I we present the energy differences between FM and AFM configurations for the various Mn substitutions.

In all these cases, the Zn ions do not attain any magnetic moment. On the other hand, the oxygens which are nearest neighbors to the Mn atoms get polarized. Their magnetic moments follow the polarization of the neighboring Mn ions and align parallel to the magnetic moments of the neighboring Mn ions in both the FM and the AFM configurations of the Mn ions. In the FM case, the largest polarization of the O ions is found for those O-ions which are mediating the coupling of two neighboring Mn ions. These O-ions however loose their polarization in the AFM case. A similar picture was also found in the case of the cationic co-doping, namely in the case of $Zn(Co-Cu-Co)O$ case[38], as well as in the case of $Ga(Mn-Cu-Mn)N$[39,40].

It should be noted that in the *far* case the FM and AFM configurations tend to become isoenergetic while in the *near* case the AFM prevails over the FM (not shown in Table I). Quite interesting appears to be the *far* case of the four Mn atoms, for which we found a tendency for the FM configuration. A particularly interesting *far* case consists of the configuration Mn-O-Zn-O-Mn-O-Zn-O-Mn-O-Zn-O-Mn, i.e., a chain of alternating cations Mn and Zn. For this case, the FM configuration of the Mn atoms is found to be more favorable than the AFM one by 0.56 meV per unit cell. However, a spin configuration of the Mn atoms of this chain consisting of FM parts which are antiferromagnetically aligned with respect to each other (i.e., $(\uparrow\uparrow\downarrow\downarrow)$) appears to be energetically more favorable. We attribute the prevailing of this type of the AFM spin configuration to the low level of the polarization of the O-ions mediating or neighboring the Mn ions. As a result the O-ions are unable to develop an effective FM coupling between the tetrahedra which provide the magnetic moments (see discussion below).

In Fig. 3 we show plots of the spin polarized total DOS of the undoped ZnO along with the total DOS of the Mn_x, x=1, 2, 3, 4 doped systems. An examination of the DOS indicates a transition from insulating to half-metal as the concentration of Mn increases. Specifically, it is observed that a sub-band starts developing near the Fermi energy (E_F) (taken to be at zero energy) which gets larger as the concentration of the Mn ions increases. At the same time the valence band is shifted to lower energies. In order to check the character of this sub-band, we plot in Fig. 4 the PDOS of the $Mn(3d)$ states and that of the $O(2p)$ states with the latter derived from the O-ions (located between Mn ions for x>1) which bond to the Mn ions. From this figure, it becomes apparent that the sub-band near the E_F is formed by $Mn(3d)$ states and $O(2p)$ states derived from O-ions which bond to Mn. This indicates that upon their spin-polarization, the O-ions which bond to Mn ions undergo a hybridization which results in the promotion of the $O(2p)$ states near E_F. Our results are in excellent agreement with the corresponding results derived by Chanier *et al.*[41]. As will be shown in the next section, this trend is also found in the case of the anionic co-doped $Zn(Mn,X)O$; X=C, N, P and S systems. Furthermore, as will be discussed in the next sections, it is this spin density of the polarized O-ions and/or the X-anion co-dopants which plays a crucial role in developing the FM coupling among the Mn-ions.

The results of this section reconfirm the trends we observed in the case of the cationic co-doping discussed in a recent report[39,40]. I.e., we find the formation of magnetic unit cells (MUCs) centered at the Mn sites which provide the magnetic moments and coupled magnetically (in a FM or AFM way) by the mediating spin density provided by the mediating co-dopants as well as the nearest neighbor O-ions[42].

IV.   MAGNETIC PROPERTIES OF CO-DOPED ZN(MN,X)O, X=C, N, P AND S

A.   Induced Magnetic Moments

We next investigated the effect of the anion co-doping on the magnetic features of Zn(Mn-X-Mn)O, X=O, S, C, N, P. In particular, we investigated the effect of the anion X co-doping on the magnetic moment, μ_{Mn}, of two nearest neighbors (nn) Mn co-dopants mediated by the X-anion. In Fig. 5 we show the schematic configuration for the Mn-X-Mn bonding and the three O atoms attached to each Mn. Our results are shown in Table II. Along with the μ_{Mn} values we also include in Table II the magnetic moments induced on co-dopant X and the O atoms bonded to each Mn. As seen in the table, the induced magnetic moments on the oxygen and sulfur anions mediating the two Mn-ions are very small. The behavior of these two elements are very similar. By contrast, however, the magnetic moment, μ_X, induced on the rest of the X-anions is quite large. Our calculations show the FM configuration to be energetically favored for X=C, N and P, while AFM is favored for X=O and S.

In the FM case, the largest μ_X value is found for the C co-dopant when aligned anti-parallel to μ_{Mn}. The magnetic moments of X=N and X=P anions are much smaller than that of $\mu_{X=C}$, while also aligned anti-parallel to μ_{Mn}. In most (if not all) of the cases, however, the induced magnetic moments on the nn O-anions align parallel to μ_{Mn}. In the AFM case, the magnetic moment, μ_X, of the anion co-dopant gets smaller and approaches the zero value for the X=C, P, O, S cases. This obviously can be attributed to the opposite polarization the anti-parallel Mn atoms impose on their mediating anion X which attempts to get a balanced state in the field of the two Mn atoms. It is quite interesting to note that, contrary to C, P, O and S, the N atom retains much of its magnetic moment value in the AFM state.

We have also considered the case of a two C atom co-doping in ZnO doped with three Mn's, namely the Zn(Mn-C-Mn-C-Mn)O case (not shown here). In this case we find that the orientation as well as the absolute value of the magnetic moments of the C anions do not change significantly when the spins on the three Mn's go from the FM ($\uparrow\uparrow\uparrow$) to the AFM ($\uparrow\uparrow\downarrow$) configurations. This is an interesting observation as it reveals a synergistic action over the Mn-C chain as its size increases.

The AFM alignment between Mn and N in ZnO was also found by Wang et $al.$[24] who showed that Mn and N like to exist as nearest neighbors in ZnO; the resulting hybridization between N(2p) and Mn(3d) orbitals was found to be the cause of a FM ground state. This was attributed to the polarization the Mn atoms impose on the N atoms with the latter in AFM orientation with respect to its Mn neighbors. Our findings are also in agreement with the report of Ye et $al.$[43] who found that in Zn(Cu)O the magnetic moments are localized within each CuO_4 tetrahedron in which a ferromagnetic coupling between Cu and O is developed.

Comparing the present results for the anionic co-doping with those of the cationic co-doping, it is observed that in both cases the magnetic moments are provided by groups of atoms forming what we termed as MUCs[42]. In the case of ZnO they take the form of tetrahedra, each of which is centered at a magnetic impurity and includes, in addition, the first nearest neighbor to the magnetic impurity O-ions. The difference we find between the anionic co-doping as compared to the cationic one is that in the latter the induced magnetic moments on non-magnetic co-dopants as well as on the first nearest neighbors of the magnetic impurities are much larger.

B.   Magnetic interactions

From Table III, it is observed that the AFM magnetic interaction between the Mn-ions, which is established for X=O (case with no co-dopants) and for X=S, changes into an FM one for X=C, N and P cases. This feature seems to be independent of the $U_{p;X}$ values used in the calculations for the co-dopants as can be seen in Table III where the the sign of E_{FM}-E_{AFM} remains the same for $U_{p;X}$=0 as well as for $U_{p;X} \neq 0$. This is an interesting result since in all cases studied (i.e., for X=O, S, N, C and P), we find the development of a hybridized Mn(3d)-X(2p) spit band near E_F. According to Chanier et $al.$[41], this split-band indicates a localization of the hole state which prevents the development of ferromagnetism as it can trap the hole states. The AFM coupling among Mn-ions in the case of X=O and at low Mn-concentration ($\leq 25\%$) could then be attributed to the localization of the hole states[41]. In view of our results and the arguments of Ref.[41], the AFM coupling should therefore have prevailed for X=C, N, and P cases as well, since these co-dopants also exhibit the hybridized split band near E_F. This, however, is not the case and instead in these systems we find that ferromagnetism prevails. This suggests that the split-band should not be considered the cause for the prevention of ferromagnetism. As will be discussed in the following, the magnetic coupling between the localized magnetic moments can be seen as that between spin polarized tetrahedra which are centered at each of the magnetic impurities and/or the co-dopants and include their first nearest neighbors.

C. Electron DOS

In Fig. 6 we present the projected electron density of states (DOS) for the systems Zn(Mn-X-Mn)O, X=O, S, N, C, P. A number of interesting features seen in these figures are worth mentioning. In particular:

1. A considerable overlap of the Mn($3d$) and X($2p$); X=O, S, N, C, P projected DOS is observed. The anion codopant p-band is split at E_F and so is the Mn($3d$). This is an indication of possible strong hybridization between these orbitals. Furthermore, both split parts of the anion p-DOS for spin-down electrons are below E_F for all codopant anions (X= S, N, C, P). Breaking it further down it can be seen that:

   - Group IV elements (C) have both split parts for the spin-up p-DOS above E_F.
   - Group V elements (N,P) have one split part of the spin-up p-DOS above E_F and the other below E_F.
   - Group VI elements (O,S) have both split parts of the spin-up p-DOS below E_F.

2. For X=O (no dopants case) there is no split in the anion p-band (as well as of Mn($3d$)) at E_F. In this case, the top of the valence band is formed mainly by O($2p$) states (see Fig. 7). On the contrary, upon doping with Mn a sub-band of O($2p$) states of the O-anion which bonds to Mn atoms is shifted closer to E_F due to its hybridization with Mn($3d$) states (see Fig. 6, top-left panel) with the latter appearing to follow the move of the O(2p) states. That is, in the Mn-doped ZnO, the O($2p$) PDOS on O-ions which are nn of the Mn atoms exhibits a narrow sub-band near E_F with an Mn($3d$) subband. In other words, the Mn-induced spin polarization of the nearby O-ions is accompanied by the O($2p$) DOS promotion to E_F.

   Further enhancement of a $2p$-orbitals derived contribution at E_F is found in the co-doped systems Zn(Mn,X)O, X=S, N, P when compared to the Zn(Mn)O case (see Fig. 6). In the case of X=N, P, and C, the spin-up part of the X($2p$) subband splits into two impurity bands which are shifted to higher energies. For X=C the impurity bands are above E_F; for X=N one impurity band is at E_F and the other above it; for X=P one of the impurity bands is just below and the other just above E_F. No corresponding spin-down bands are found in this or lower range of energies. Only for the case X=P do we find that the spin-down impurity band is split into two subbands at energies lower than the appearance of the spin-up impurity bands. A very interesting point emerging from Fig. 6 is that both the spin-up impurity X($2p$) states near E_F are followed by a corresponding spin-up states of Mn($3d$). It appears that as the Mn($3d$) (and correspondingly the X($2p$)) states undergoes a shifting and splitting process, it drags along with itself the X($2p$) (and correspondingly the Mn($3d$)) states in such a way that the Mn($3d$) and X($2p$) states split and shift as one orbital state.

3. The anion vacancy appears to create a defect band below E_F which results in the reduction of the gap.

4. There appears to be a significant change in the energy gap value as the X-anion is changed. The largest gap is observed for X=O and the smallest for X=P for which the impurity bands are much broader due, perhaps, to the larger Mn-P induced lattice disturbances compared to the other Mn-X ones (see Table III).

The results of the projected DOS indicate that the anion X($2p$) and those of the polarized O($2p$) as well as the cation Mn($3d$) states are strongly coupled and hybridized. Interestingly, at E_F, this coupling refers to the spin-up states for both the anions X($2p$) and the Mn($3d$) for X= N and P. For the polarized O-ions, however, the coupling refers to both spin-states. In the case of X=S we observe that at E_F the contributed states come from spin-up Mn($3d$) and spin-down S($2p$) states. It is worth noting that, contrary to the findings of Wang *et al.*[24], our results for N co-doping of Zn(Mn)O indicate contribution of both N($2p$) and Mn($3d$) spin-up states at E_F. It is only for the case of C co-doping that we do not find contribution of states at E_F coming from either the C($2p$) or the Mn($3d$) states.

Also, while the additional holes introduced in the system by the dopants are expected to lead to metallic states, we do not find this to be the case. This is likely due to the small dopant concentration which results in the formation of atomic-like states rather than extended impurity bands.

D. Electronegativity of Anions and Atomic Magnetic Moments

Recently, Yang *et al.*[44] reported *ab initio* computational results on the magnetic features of the II-VI and III-V semiconductors doped at anion sites. Their results indicated a direct correlation between the magnetic moment of the cations and the electronegativity of the anion dopants. In particular, they found an increase in the cationic magnetic moments with a decrease in the electronegativity of the nearby anion dopants.

We have investigated this trend in the present work for the co-doped systems Zn(X)O; X=C, N, P, S, and our results are shown in Table III. The Table also includes the case when X represents an anion vacancy. It is apparent from

Table III that the correlation between μ_{Mn} and anion electronegativity as stated by Yang *et al.*[44] is not applicable in the systems we studied. The magnetic moment of the Mn co-dopant, μ_{Mn}, does not follow the electronegativities of the listed series of the the anion-dopants. Instead, an opposite trend is observed and despite the fact that the electronegativities of both Zn and Mn are approximately the same (1.55 and 1.65, respectively). That is, the magnetic moment of the Mn atoms is found (with the exception of P) to *increase* with an increase in the electronegativity of the neighboring anions. On the other hand, we observe that μ_{Mn} correlates well with the total valence charge Q_{Mn} of Mn indicating a rather strong dependence of the cation magnetic moment on the charge transfer which follows the anion doping.

V. DISCUSSION AND SUMMARY

We have performed a detailed investigation of the effect of the anionic co-doping on the magnetic properties of the DMSs doped with transition metal (TM) ions. The present work refers to the anionic co-doping of Zn(Mn,X)O, X=O, S, C, N and P. Our findings are in complete analogy with corresponding results for the cationic co-doping of Zn(TM$_1$,TM$_2$)O as studied in our earlier works[38–40]. For both, the cationic and anionic co-dopings we find that the magnetic impurities induce magnetic moments on their nearest neighbors with the largest induced magnetic moment observed on the cation or the anion which mediates two magnetic impurities.

In the anionic co-doping, the Mn ions in ZnO polarize their nn O-anions and induce magnetic moments on them which are all aligned parallel to the magnetic moment of the Mn. This appears to be the case when the Mn atoms are coupled via an S-anion. However, if two Mn ions are coupled by an anion X different than O and S (more specifically if X=C, N and P), the induced magnetic moment on X aligns antiparallelly to that of Mn (in the Mn-Mn FM coupling configuration). In the AFM configuration of two Mn coupled by an anion X=O, S, C and P, the magnetic moment induced on X is found to be approximately zero. For X=N, $\mu_{\mathrm{X=N}}$ does not become zero. These findings are analogs of the *double exchange* and *superexchange* magnetic couplings. On the other hand, in the cationic co-doping of ZnO and/or GaN with TMs, we have found[39,40] that magnetic moments are induced on the TM co-dopants and the FM/AFM coupling between two magnetic impurities appears as the FM/AFM coupling of the tetrahedra that are centered at each co-dopant. The magnetic coupling in this case appears as a magnetic coupling among these tetrahedra. We term these FM/AFM couplings the *grand double exchange* and *grand superexchange*, respectively, in order to emphasize the difference between the classically well known atomic type double-exchange and superexchange interactions from the synergistic *molecular* type of interaction which is developed between the polarized tetrahedra.

The development of the magnetic coupling through polarized tetrahedra is reminiscent of a molecular type of interaction which originates in the overlap between MOs with significant contributions in more than one neighboring polarized tetrahedra. This is in excellent agreement with our earlier findings and proposal on the magnetic interaction among the magnetic moments formed by C-vacancies in the C$_{60}$-based polymers and was attributed to the *remote overlap* of the MOs[42,45]. This is a more general picture of a mediated interaction that is based on the synergistic action between two co-dopants; one that is responsible for providing the magnetic moments (and this could also be a TM magnetic impurity) and the other that provides or facilitates the FM coupling among the magnetic moments. In view of this, co-doping appears to be a potential mechanism that can be used to justify the defect-induced magnetism in DMSs on a more realistic basis.

* Electronic address: `slisenk@usf.edu`

† Electronic address: `andriot@iesl.forth.gr`

‡ Electronic address: `rmshee0@email.uky.edu`

§ Electronic address: `madhu@ccs.uky.edu`

[1] T. Dietl, H. Ohno, F. Matsukura, J. Cibert, and D. Ferrand, Science **287**, 1019 (2000).

[2] H. Ohno, D. Chiba, F. Matsukura, T. Omiya, E. Abe, T. Dietl, Y. Ono, and K. Ohtani, Nature **408**, 944 (2000).

[3] Lqandolt-Bornstein, *Condensed Matter* (Springer-Verlag, Heidelberg, 2002).

[4] D. C. Look, R. Jones, J. Sizelove, N. Garces, N. Giles, and L. Haliburton, Phys. Solid State **195**, 171 (2003).

[5] N. A. Hill and U. V. Waghmare, Phys. Rev. B **62**, 8802 (2000).

[6] P. Gopal and N. A. Spaldin, J. Electron. Mater. **35**, 538 (2006).

[7] K. Ueda, H. Tabata, and T. Kawai, Appl. Phys. Lett. **79**, 988 (2001).

[8] M. Venkatesan, C. B. Fitzgerald, J. G. Lunney, and J. M. D. Coey, Phys. Rev. Lett. **93**, 177206 (2004).

[9] T. Fukumura, Z. Jin, A. Ohtomo, H. Koinuma, and M. Kawasaki, Appl. Phys. Lett. **75**, 3366 (1999).

[10] S. J. A. S. Jung, G. C. Yi, C. Jung, S. I. Lee, and S. Cho, Appl. Phys. Lett. **80**, 4561 (2002).

[11] P. Sharma, A. Gupta, K. V. Rao, F. J. Owens, R. Sharma, R. Ahuja, J. M. Osorio-Guillen, and G. A. Gehring, Nat. Mater **2**, 673 (2003).

[12] C. Song, K. W. Geng, F. Zeng, X. B. Wang, Y. X. Shen, F. Pan, Y. N. Xie, T. Liu, H. T. Zhou, and Z. Fan, Phys. Rev. B **73**, 024405 (2006).

[13] K. R. Kittilstved, N. S. Norberg, and D. R. Gamelin, Phys. Rev. Lett. **94**, 147209 (2005).

[14] M. S. Park and B. I. Min, Phys. Rev. B **68**, 224436 (2003).

[15] K. Sato and H. Katayama-Yoshida, J. Appl. Phys. **39**, L555 (2000).

[16] L. M. Sandratskii and P. Bruno, Phys. Rev. B **73**, 045203 (2006).

[17] N. A. Spaldin, Phys. Rev. B **69**, 125201 (2004).

[18] L. Petit, T. C. Schulthess, A. Svane, Z. Szotek, W. M. Temmerman, and A. Janotti, Phys. Rev. B **73**, 045107 (2006).

[19] E. C. Lee and K. J. Chang, Phys. Rev. B **69**, 085205 (2004).

[20] Y. W. Heo, M. P. Ivill, K. Ip, D. P. Norton, and S. Pearton, Appl. Phys. Lett. **84**, 2292 (2003).

[21] Y. W. Yoon, S. B. Cho, S. C. We, B. J. Yoon, S. Suh, S. H. Song, and Y. J. Shin, J. Appl. Phys. **93**, 7879 (2003).

[22] P. Sati, R. Hyan, R. Kuzian, S. Regnier, S. Schafer, A. Stepanov, C. Morhain, C. Deparis, M. Laugt, M. Goiran, et al., Phys. Rev. Lett. **96**, 017203 (2006).

[23] J. R. Neal, A. J. Behan, R. M. Ibrahim, H. J. Blythe, M. Ziese, A. M. Fox, and G. A. Gehring, Phys. Rev. Lett. **96**, 197208 (2006).

[24] Q. Wang, Q. Sun, P. Jena, and Y. Kawazoe, Phys. Rev. B **70**, 052408 (2004).

[25] P. Gopal and N. A. Spaldin, Phys. Rev. B **74**, 094418 (2006).

[26] R. Janisch, P. Gopal, and N. A. Spaldin, J. Phys.: Condens. Matter **17**, R657 (2005).

[27] M. H. F. Sluiter, Y. Kawazoe, P. Sharma, A. Inoue, A. R. Raju, C. Rout, and U. V. Waghmare, Phys. Rev. Lett. **94**, 187204 (2005).

[28] M. K. Yadav, B. Sanyal, and A. Mookerjee, J. Magn. Magn. Mater. **321**, 273 (2009).

[29] X. C. Liu, E. W. Shi, , Z. Z. Chen, H. W. Zhang, B. Xiao, and L. X. Song, Appl. Phys. Lett. **88**, 2503 (2006).

[30] X. H. Xu, H. J. Blythe, M. Ziese, A. J. Behan, J. R. Neal, A. Mokhtari, R. M. Ibrahim, A. M. Fox, and G. A. Gehring, New Jourbal of Physics **8**, 135 (2006).

[31] N. Theodoropoulou, V. Misra, P. Lechair, G. P. Berera, J. S. Moodera, B. Satpati, and T. Som, J. Magn. Magn. Mater **300**, 407 (2006).

[32] J. P. Perdew, K. Burke, and M. Ernzerhof, Phys. Rev. Lett. **77**, 3865 (1996).

[33] S. L. Dudarev, G. A. Botton, S. Y. Savrasov, C. J. Humphreys, and A. P. Sutton, Phys. Rev. B **57**, 1505 (1998).

[34] G. Kresse and J. Hafner, Phys. Rev. B **47**, 558 (1993).

[35] G. Kresse and D. Joubert, Phys. Rev. B **59**, 1758 (1999).

[36] P. E. Blöchl, Phys. Rev. B **50**, 17953 (1994).

[37] L. B. Duan, G. H. Rao, C. Y. Wang, J. Yu, and T. Wang, J. Appl. Phys. **104**, 013909 (2008).

[38] N. N. Lathiotakis, A. N. Andriotis, and M. Menon, Phys. Rev. B. **78**, 193311 (2008).

[39] S. Lisenkov, A. N. Andriotis, and M. Menon, Phys. Rev. B **82**, 165454 (2010).

[40] A. N. Andriotis, S. Lisenkov, and M. Menon, J. Phys.: Condens. Matter **23**, 086004 (2011).

[41] T. Chanier, F. Virot, and R. Hayn, Phys. Rev. B **79**, 205204 (2009).

[42] A. N. Andriotis, R. M. Sheetz, N. N. Lathiotakis, and M. Menon, Int. J. Nanotechnology **6**, 164 (2009).

[43] L. H. Ye, A. J. Freeman, and B. Delley, Phys. Rev. B **73**, 033203 (2006).

[44] K. Yang, R. Wu, L. Shen, Y. P. Feng, Y. Dai, and B. Huang, Phys. Rev. B **81**, 125211 (2010).

[45] A. N. Andriotis, M. Menon, R. M. Sheetz, and L. Chernozatonskii, Phys. Rev. Lett **90**, 026801 (2003).

	Schematic bonding	$E_{\mathbf{FM}}$-$E_{\mathbf{non\text{-}FM}}$	ΔE (meV)
2Mn	Mn-O-Mn	E(↑↑)-E(↑↓)*	35.68
	Mn-O-Zn-O-Zn-O-Mn	E(↑↑)-E(↑↓)	0.30
3Mn	Mn-O-Mn-O-Mn	E(↑↑↑)-E(↓↑↑)*	67.80
		E(↑↑↑)-E(↑↓↑)	32.37
	Mn-O-Zn-O-Mn-O-Mn	E(↑↑↑)-E(↑↓↑)	36.15
		E(↑↑↑)-E(↓↑↑)	0.0
4Mn	Mn-O-Mn-O-Mn-O-Mn	E(↑↑↑↑)-E(↑↓↑↓)*	101.16
		E(↑↑↑↑)-E(↑↑↓↓)	31.93
	Mn-O-Mn-O-Zn-O-Mn-O-Mn	E(↑↑↑↑)-E(↑↓↑↓)	81.53
		E(↑↑↑↑)-E(↑↑↓↓)	-0.14
	Mn-O-Zn-O-Mn-O-Zn-O-Mn-O-Zn-O-Mn	E(↑↑↑↑)-E(↑↓↑↓)	-0.56
		E(↑↑↑↑)-E(↑↑↓↓)	0.16

TABLE I: Energy differences, ΔE, between various spin-configurations of Zn(Mn$_k$)O, k =1,2,3,4. Positive values of ΔE indicate stability of the non-FM spin-configuration. Asterisk indicates the most stable spin configuration for each k.

Spin configuration	Dopant		Mn1				Mn2			
FM		X	O1	O2	O3	Mn1	O4	O5	O6	Mn2
	C	-0.499	0.011	0.009	0.010	4.292	-0.008	0.001	-0.008	4.302
	N	-0.260	0.008	0.047	0.008	4.427	0.028	-0.019	0.028	4.405
	P	-0.213	0.004	0.039	0.004	4.484	-0.001	-0.010	-0.001	4.450
	S	0.025	0.031	0.037	0.031	4.610	0.029	0.032	0.029	4.609
	O	0.064	0.030	0.035	0.030	4.631	0.029	0.030	0.029	4.630
	Vac		0.034	0.006	0.033	4.603	0.044	0.030	0.040	4.623
AFM	C	-0.008	0.008	0.002	0.008	4.324	0.022	-0.026	0.021	-4.308
	N	0.198	0.031	0.034	0.031	4.607	-0.001	0.014	-0.001	-4.102
	P	-0.058	0.012	-0.001	0.000	4.495	0.014	-0.048	0.019	-4.452
	S	-0.008	0.030	0.029	0.030	4.602	-0.028	-0.029	-0.028	-4.600
	O	-0.004	0.030	0.025	0.030	4.625	-0.029	-0.030	-0.029	-4.624
	Vac		0.034	-0.003	0.033	4.603	-0.021	-0.030	-0.027	-4.624

TABLE II: Magnetic moments (in μ_B) of the two nn Mn-ions, their mediating X ion (X=C, N, P, S and O or an anion vacancy, Vac) and the O atoms bonded to Mn's in the FM and AFM states. Each row lists the magnetic moments of X, O's and Mn's when X=element on the left. The schematic bonding configuration used in this Table is shown in Fig. 5.

Dopants (Mn-X-Mn)	Mn-O-Mn	Mn-S-Mn	Mn-N-Mn	Mn-C-Mn	Mn-P-Mn	Mn-Vac-Mn
Electronegativity (X)	3.44	2.58	3.04	2.55	2.19	
FM-case						
μ_X	0.064	0.025	-0.260	-0.499	-0.222	
μ_{Mn_1}	4.630	4.610	4.427	4.292	4.465	4.603
μ_{Mn2}	4.631	4.609	4.405	4.302	4.487	4.623
AFM-case						
μ_X	-0.004	-0.008	0.198	0.008	-0.058	
μ_{Mn_1}	4.625	4.602	4.607	4.324	4.580	4.623
μ_{Mn2}	-4.624	-4.600	-4.102	-4.308	-4.367	-4.624
FM-case Charge (Q_{Mn_1})	11.442	11.447	11.464	11.396	11.456	11.390
Charge (Q_{Mn_2})	11.443	11.439	11.469	11.387	11.439	11.453
Charge (Q_X)	5.099	3.873	3.708	2.276	2.674	
E_{FM}-E_{AFM} (meV)	+35	+20	-211	-598	-199	-4
		(+19)	(-240)	(-440)	(-390)	
Mn-X distance (Å)	1.99	2.38	1.97,1.99	1.99	2.40,2.36	

TABLE III: Magnetic moments (in μ_B) on the two nn Mn atoms of the systems Zn(Mn-X-Mn)O; X=O, S, N, C and P in the FM and AFM Mn-spin configuration. The results for Zn(Mn-X-Mn)O; X=vacancy are also included. The atomic charge Q is the valence charge within the Wigner-Seitz (WS) radii; within the pseudopotential approximation employed with the valence electrons consisting of $3p^6$, $4s^2$ and $3d^5$ electrons. The present data indicate a trend in the correlation between the magnetic moments of the Mn atoms and the electronegativity of the X atom mediating them which is opposite to the one expected from the findings of Ref.[44]. On the other hand, our data shows proportionality of the variation of the total valence charge of the Mn atoms with the electronegativity of their mediating X atoms. The numbers in parenthesis denote E_{FM}-E_{AFM} values for $U_p \neq 0$ for S, N, C and P.
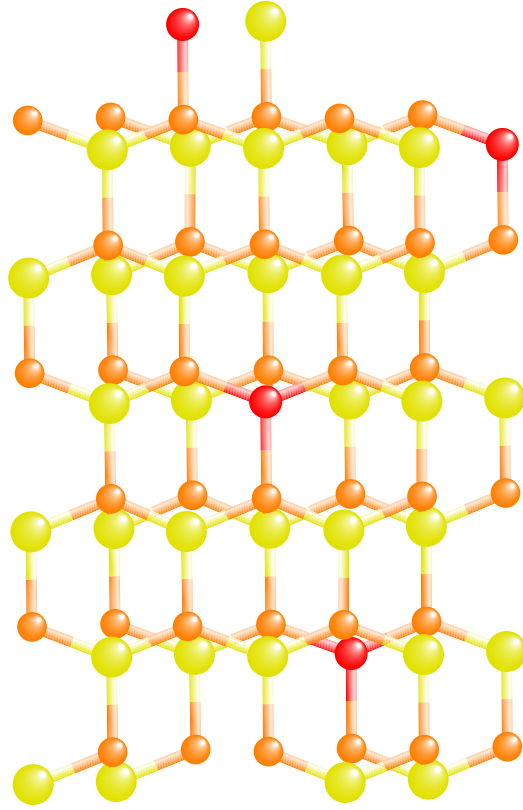
FIG. 1: Figure illustrating a 72 atom wurzite supercell of ZnO with 4 Mn ions (shown in red) in "far" configuration. The Zn atoms are shown in yellow and O in orange.
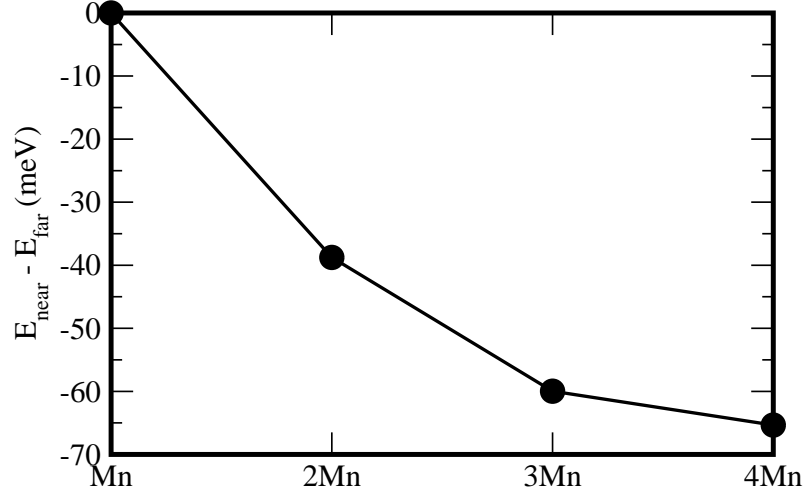
FIG. 2: Calculated energy difference, $\Delta E = E_{near} - E_{far}$, for substitutional Mn atoms. The negative energy difference indicates that Mn atoms prefer to cluster together.

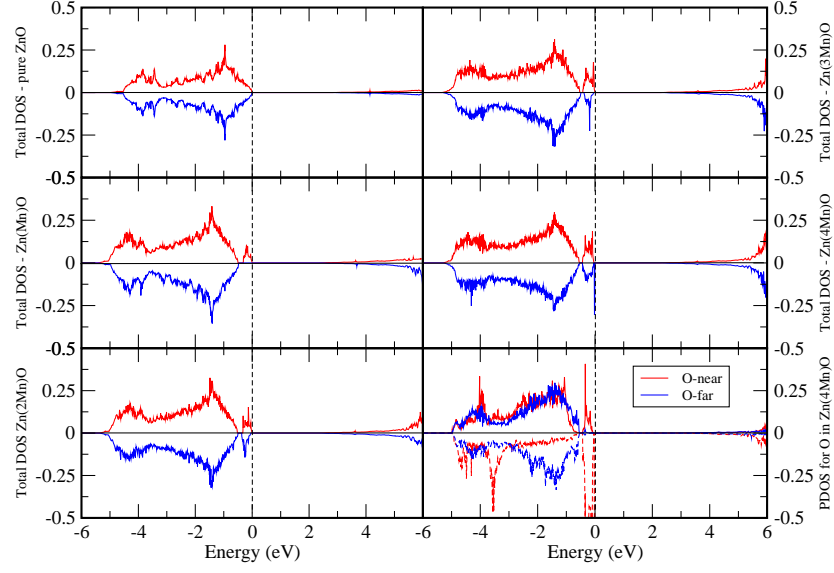FIG. 3: Total DOS for ZnO and DOS and PDOS for Zn(Mn$_x$)O. Spin up is indicated as positive (in red) and spin down as negative (in blue), except for the bottom right panel. In the latter the (positive) solid lines indicate spin up and the (negative) dashed lines indicate spin down.

FIG. 4: PDOS for Zn(Mn$_x$)O, x=1,2,3,4. Positive values indicate spin up and negative ones indicate spin down PDOS's for each color.
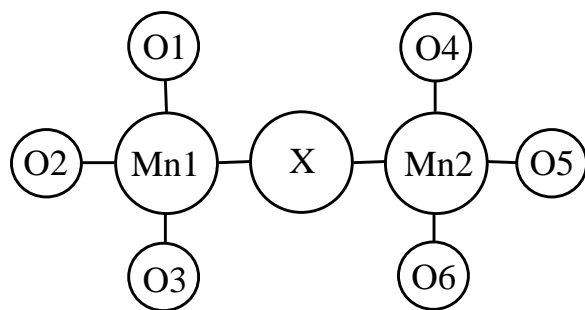
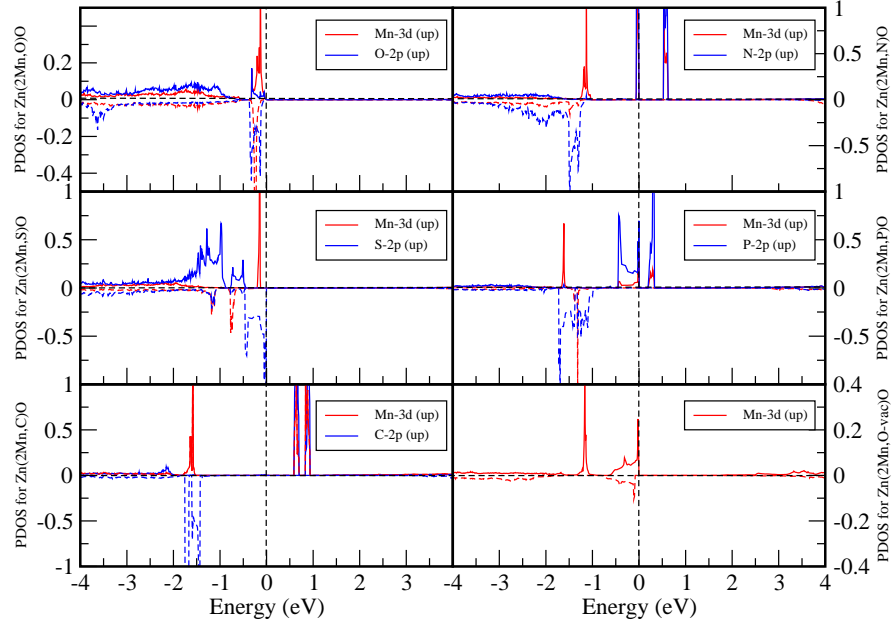FIG. 5: Schematic bonding configuration Mn1-X-Mn2 used in Table II.

FIG. 6: PDOS for the systems Zn(Mn-X-Mn)O with X being one of the anions; O, N, S, C and P or an anion vacancy in the FM Mn-spin configuration. Positive values indicate spin up, while negative ones indicate spin down PDOS's for each color.
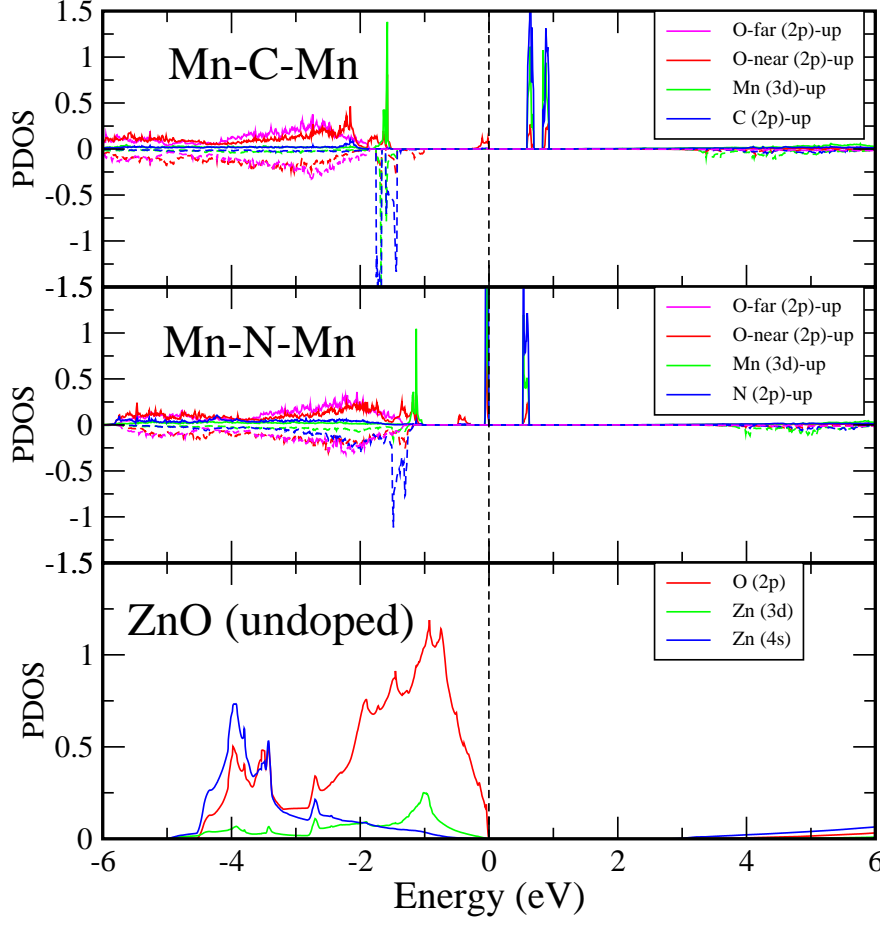
FIG. 7: PDOS for Zn(Mn,X)O, X=N, C indicating the induced O(2p) DOS at E$_F$ as a result of their spin polarization due to the magnetic ions. Positive values indicate spin up and negative ones indicate spin down DOS's for each color. The bottom panel contains the spin-up PDOS (which is identical to the spin-down one) for undoped ZnO for comparison.